Multiple metal binding domains enhance the Zn(II) selectivity of the divalent metal ion transporter AztA

Tong Liu[1], Hermes Reyes-Caballero[1], Chenxi Li[2], Robert A. Scott[2], and David P. Giedroc[1]*

SUPPPORTING INFORMATION

Supplementary Methods

Supplementary Table SI
Sedimentation equilibrium analysis of Zn(II) and Cd(II) loaded $AztA^{aHbH}$

Supplementary Table SII
EXAFS curve-fitting results.

Supplementary Table SIII
$^{1}H_{N}$ and ^{15}N, $^{13}C\alpha$ and $^{13}C\beta$ resonance assignments for apo-$AztA^{aH}$ (25 ºC, pH 6.5)

Supplementary Figure S1
HPLC size exclusion chromatographic analysis of apo, Zn_1 and $Cd_{0.5}$ forms of $AztA^{aH}$

Supplementary Figure S2
Overlay of ^{1}H-^{15}N HSQC spectra acquired for apo-$AztA^{aH}$ and apo-$AztA^{aHbH}$ (25 ºC, pH 6.5)

Supplementary Figure S3
Chemical shift difference plots (Δppm vs. residue number) for (**A**) apo-$AztA^{aH}$ – apo-$AztA^{aHbH}$ and (B) apo-$AztA^{aH}$ – Zn_1-$AztA^{aH}$

Supplementary Figure S4
Subsection of the random coil region of ^{1}H-^{15}N HSQC spectra acquired for apo-$AztA^{aH}$ and Zn_1-$AztA^{aH}$

Supplementary Figure S5
Electrostatic surface potential renderings of homology models of the a-MBD and b-MBD of AztA

SUPPLEMENTARY METHODS

Equilibrium analytical ultracentrifugation. Six channel cells containing 10 μM apo AztA^{aHbH} or 20 μM AztA^{aH} in buffer C with or without addition of 1.0 mol equiv Cd(II), Pb(II), or 1.0 and 2.0 mol equiv of Zn(II) were assembled in the anaerobic globe box and spun at 25,000, 31,000 and 41,000 rpm in an An-60Ti rotor in an XL-A Beckman Optima analytical ultracentrifuge at 25 ºC until equilibrium was reached. Scans at 25,000 rpm were chosen for detailed analysis. The absorbance was simultaneously acquired at 240, 235 and 230 nm and was globally analyzed using a simultaneous fitting routine in Ultrascan 9.0 (UTHSCSA) to a single component ideal species model or to a multiple non-interacting component species model, the latter of which gives the relative concentrations of each non-interacting species. An input partial specific volume of 0.7141 mL/g as calculated by Sednterp was used with a buffer density of 1.0 mg/ml used to estimate the molecular weight. All fits revealed a dominant monomeric species (MW_{exp}= 23,554 D for apo-AztA^{aHbH}) with an acceptable variance and random residuals (fits not shown).

Size exclusion chromatography. 10-20 μM samples of AztA^{aH} with the indicated metal:protein ratio were incubated for ≥12 h and loaded on a 10/300GL Superdex-75 gel filtration column (Amersham Biosciences) on an Äkta HPLC system (Amersham Biosciences). The column was run at 0.4 mL/min in buffer C with 2 mM DTT. Molecular weight calibration of the column was conducted with a mixture of standard proteins (cytochrome C, myoglobin, ovalbumin, bovine serum albumin) chromatographed in the same buffer and at the same flow rate.

Dynamic light scattering measurements. Dynamic light scattering experiments were carried out using a Zelasizer NanoS instrument (Malvern Instruments). Apo- or metal -loaded

$AztA^{aH}$ solutions at 5-20 μM in buffer C were first filtered through a 0.2 μm filter and subjected to light scattering analysis at 25 ºC. Intensity and volume distribution analysis was determined from the value of the diffusion coefficient (D_{25}) using the software provided by manufacturer.

EXAFS Curve-fitting. Feff 8.2 (*1*) was used to generate scattering functions for M-N, M-S shells (M = Cd, Zn). For each sample, MN_xS_{4-x} (x = 0-4) fits are compared in Supplementary Table SII. For some fits with x = 1, the M-N Debye-Waller factor was fixed to a reasonable value (σ_{as}^2 = 0.0020 Å^2). Best fits were chosen based on (a) chemically reasonable M-N and M-S bond distances; (b) physically reasonable M-N and M-S Debye-Waller factors; (c) ΔE_0 values near zero; (d) low f' values; and (e) bond valence sum (BVS) (*2*) values near 2.0, the valence of Cd(II) and Zn(II). The chosen best fits for each sample are highlighted in red font in Supplementary Table SII. For comparison, we have provided analogous curve-fitting results for known MS_4 sites ([Zn]- (*3*) and [Cd]- *Clostridium pasteurianum* rubredoxins (*4*)) and known $M(N,O)_1S_3$ sites ([Zn]human TFIIB (*5, 6*) and [Cd]CadA-NTK (*6*)).

SUPPLEMENTARY TABLE SI: Sedimentation equilibrium analysis of Zn(II) and Cd(II) loaded $AztA^{aHbH}$.[a]

Equilibrium parameter	Zn_1 $AztA^{aHbH}$	Zn_2 $AztA^{aHbH}$	Cd_1 $AztA^{aHbH}$	Pb_1 $AztA^{aHbH}$
MW (fitted) (D)[b]	23,900	24,570	24,260	23,250
variance[c]	8.13e-05	4.20e-05	3.82e-05	5.16e-05

[a]25,000 rpm, buffer C, 25 (±0.1) ºC monitored at 240, 235 and 230 nm. [b]Expected molecular weight for the metal free $AztA^{aHbH}$ monomer is 23,554 D. The fitted molecular weight reflects a global analysis of equilibrium scans acquired at all three wavelengths.. [c]variance (χ^2) = ($\Sigma[f(x_i - y_i)]^2/N$), where N is the number of data points, f is the fitting function, and x_i and y_i are fitted and experimental data points, respectively.

SUPPLEMENTARY TABLE SII: Curve fitting results for Zn Cd EXAFS[a]

Sample filename (k range) $\Delta k^3\chi$	Fit	Shell	R_{as} (Å)	σ_{as}^2 (Å^2)	ΔE_0 (eV)	f[b]	BVS[c]
$Zn_{1.0}$AztA[aH]	1	Zn-S_3	2.28	0.0060	-1.20	0.122	1.80
ZA10A (2-12 Å^{-1})	2	Zn-S_4	2.28	0.0078	-2.07	0.112	2.39
$\Delta k^3\chi$ = 13.26	3	Zn-S_3	2.28	0.0042	-2.90	0.090	2.40
		Zn-N_1	1.96	-0.0020			
	4	Zn-S_3	2.29	0.0049	-1.39	0.096	2.34
		Zn-N_1	1.97	[0.0020][d]			
	5	Zn-S_2	2.29	0.0017	-0.90	0.092	2.29
		Zn-N_2	1.99	0.0015			
	6	Zn-S_1	2.31	-0.0018	0.73	0.101	2.10
		Zn-N_3	2.02	0.0032			
$Zn_{0.7}$AztA[aH]	7	Zn-S_3	2.29	0.0062	-0.39	0.121	1.75
ZA07A (2-12 Å^{-1})	8	Zn-S_4	2.28	0.0081	-1.31	0.106	2.39
$\Delta k^3\chi$ = 11.59	9	Zn-S_3	2.29	0.0046	-0.83	0.085	2.31
		Zn-N_1	1.99	-0.0012			
	10	Zn-S_3	2.30	0.0053	0.02	0.089	2.26
		Zn-N_1	1.99	[0.0020]			
	11	Zn-S_2	2.31	0.0022	0.93	0.087	2.14
		Zn-N_2	2.02	0.0015			
	12	Zn-S_1	2.34	-0.0014	5.43	0.097	1.86

		$Zn\text{-}N_3$	2.07	0.0021			
Human TFIIB	13	$Zn\text{-}S_3$	2.34	0.0023	0.79	0.090	1.53
ZHB0A (2-13 $Å^{-1}$)	14	$Zn\text{-}S_4$	2.34	0.0039	0.78	0.075	2.03
$\Delta k^3\chi$ = 14.96	15	$Zn\text{-}S_3$	2.34	0.0011	0.73	0.064	1.99
		$Zn\text{-}N_1$	2.06	-0.0026			
	16	$Zn\text{-}S_3$	2.34	0.0019	0.75	0.070	1.99
		$Zn\text{-}N_1$	2.06	[0.0020]			
	17	$Zn\text{-}S_2$	2.36	-0.0010	2.39	0.071	1.75
		$Zn\text{-}N_2$	2.09	-0.0008			
	18	$Zn\text{-}S_1$	2.38	-0.0042	5.55	0.084	1.61
		$Zn\text{-}N_3$	2.13	-0.0007			
[Zn]*Cp* rubredoxin	19	$Zn\text{-}S_3$	2.34	0.0018	-1.34	0.106	1.54
ZRDWA (2-12 $Å^{-1}$)	20	$Zn\text{-}S_4$	2.34	0.0031	-0.83	0.086	2.04
$\Delta k^3\chi$ = 17.07	21	$Zn\text{-}S_3$	2.36	0.0002	2.06	0.073	1.74
		$Zn\text{-}N_1$	2.13	-0.0051			
	22	$Zn\text{-}S_3$	2.33	0.0011	-2.04	0.102	2.39
		$Zn\text{-}N_1$	1.85	[0.0020]			
	23	$Zn\text{-}S_2$	2.38	-0.0017	4.21	0.082	2.01
		$Zn\text{-}N_2$	2.15	-0.0037			
	24	$Zn\text{-}S_1$	2.40	-0.0045	5.31	0.097	1.49
		$Zn\text{-}N_3$	2.16	-0.0031			

$Cd_{0.5}AztA^{aH}$	5	Cd-S_3	2.48	0.0034	-1.67	0.107	1.85
DT05A (2-12 $Å^{-1}$)	6	Cd-S_4	2.48	0.0052	-1.49	0.107	2.47
$\Delta k^3\chi$ = 15.07	7	Cd-S_3	2.50	0.0044	2.60	0.106	2.09
		Cd-O_1	2.31	0.0022			
	8	Cd-S_2	2.38	-0.0053	7.75	0.117	2.40
		Cd-O_2	2.24	-0.0032			
[Cd]*Cp* rubredoxin	9	Cd-S_3	2.53	0.0005	0.28	0.068	1.64
DRD0A (2-12 $Å^{-1}$)	10	Cd-S_4	2.53	0.0021	0.73	0.057	2.19
$\Delta k^3\chi$ = 12.47	11	Cd-S_3	2.54	0.0003	2.87	0.054	1.93
		Cd-O_1	2.29	-0.0003			
	12	Cd-S_2	2.43	-0.0085	10.32	0.088	2.10
		Cd-O_2	2.30	-0.0064			
[Cd]CadA-NTK	13	Cd-S_3	2.50	0.0048	-5.30	0.109	1.78
DNK0A (2-12 $Å^{-1}$)	14	Cd-S_4	2.50	0.0067	-4.92	0.106	2.37
$\Delta k^3\chi$ = 9.42	15	Cd-S_3	2.51	0.0051	-2.59	0.105	2.02
		Cd-O_1	2.33	0.0071			
	16	Cd-S_2	2.41	-0.0038	6.79	0.116	2.31
		Cd-O_2	2.24	-0.0017			

[a] Shell is the chemical unit defined for the multiple scattering calculation. Subscripts denote the number of scatterers per metal. R_{as} is the metal-scatterer distance. σ_{as}^2 is a mean square deviation in R_{as}. ΔE_0 is the shift in E_0 for the theoretical scattering functions (single value for all shells of a fit). The fits shaded in ***red*** represent best fits to the experimental data.

[b] f' is a normalized error (chi-squared) (see Table SI).

[c] Zn BVS = $\Sigma\exp[(r_o-R_{as})/B]$, *B*=0.37, r_0(Zn(II)-S)=2.090, r_0(Zn(II)-N)=1.776 (*2*).

Cd BVS = $\Sigma\exp[(r_o-R_{as})/B]$, *B*=0.37, r_0(Cd(II)-S)=2.304, r_0(Cd(II)-O)=1.904 (*2*).

[d] σ_{as}^2 values in square brackets were fixed during optimization.

SUPPLEMENTARY TABLE SIII: $^{1}H_{N}$ and ^{15}N, $^{13}C\alpha$ and $^{13}C\beta$ resonance assignments for apo-AztA^{aH} (25 ºC, pH 6.5)

Residue #	$^{13}C\alpha$	$^{13}C\beta$	^{15}N	$^{1}H_{N}$
Ser6	56.84	62.64	116.6	8.507
Leu7	54.54	42.03	123.8	7.818
Lys8	54.31	35.31	125.6	8.887
Thr9	60.95	70.98	116	8.335
Gln10	54.15	33.25	125.9	9.413
Thr11	61.1	69.4	119	8.754
Leu12	53.16	44.36	126	9.444
Gln13	54.21	29.32	123	8.833
Val14	61.04	33.07	127.5	9.071
Gly15	43.86	–	118.1	9.326
Gly16	45.2	–	106.4	8.381
Met17	57.02	35.14	118.9	8.827
Gly20	45.08	–	111	8.596
Cys22	62.34	28.09	121.6	7.724
Ala23	54.86	18.22	119	6.824
Lys24	57.59	31.22	116.7	7.279
Thr25	66.3	68.11	115.8	7.934
Ile26	65.14	38.19	121	7.796
Glu27	54.27	30.79	119.9	8.353

Val28	65.79	31.51	117.3	8.383
Ala29	54.64	18.38	120.8	7.559
Gln31	57.67	27.84	114.9	8.222
Gln32	55.42	28.9	114.1	7.395
Leu33	54.11	41.45	122.3	7.488
His34	57.39	28.63	125.6	8.767
Gly35	44.69	-	113.1	8.522
Val36	63.31	31.98	122.1	7.822
Thr37	62.17	67.91	121.3	9.151
Glu38	55.62	33.16	121.6	7.58
Ala39	51.43	22.82	124.7	8.729
Thr40	59.21	71.17	114.2	8.704
Val41	60.99	33.06	125.8	9.738
Asn42	51.25	40.12	126.3	8.451
Phe43	59.93	-	125.6	9.301
Thr44	66.83	66.84	113.1	8.01
Thr45	60.94	69.76	107.6	7.564
Gly46	45.59	-	112	7.961
Lys47	55.3	34.33	116.5	7.418
Ala48	49.12	21.48	126.8	9.488
Arg49	54.72	32.13	124.2	9.062
Val50	59.7	35.35	125.1	9.133

Ser51	56.73	64.29	122.9	9.225
Tyr52	54.94	41.41	121	9.38
Asp53	52.45	54.76	117.9	8.312
Ala54	52.53	18.59	130.1	8.682
Glu55	57.35	29.26	116.3	8.74
Val56	61.66	33.82	114.2	7.469
Leu57	53.42	45.03	124.2	8.121
Ser58	55.59	65.3	116.2	8.015
Gln59	59.34	28.82	122.9	8.878
Lys60	58.97	31.63	117.4	8.03
Ser61	61.54	62.58	114.5	7.702
Ile62	63.9	45.65	122.3	7.146
Tyr63	59.12	36.66	118.4	8.005
Asn64	55.32	37.47	116	8.663
Gln65	57.63	28.29	121.6	7.858
Ile66	65.48	38.36	117.9	7.424
Lys67	58.27	35.28	118.6	8.476
Gly68	50.16	-	107.9	8.396
Leu69	54.52	43.03	118.5	7.212
Gly70	44.18	-	104.5	7.914
Tyr71	56.95	35.79	119.7	7.983
Thr72	59.57	70.2	109.3	8.256

Ile73	59.04	38.13	119.7	8.412
Glu74	55.18	30.77	126.5	8.675
Gln75	53.1	29.8	120.3	8.48

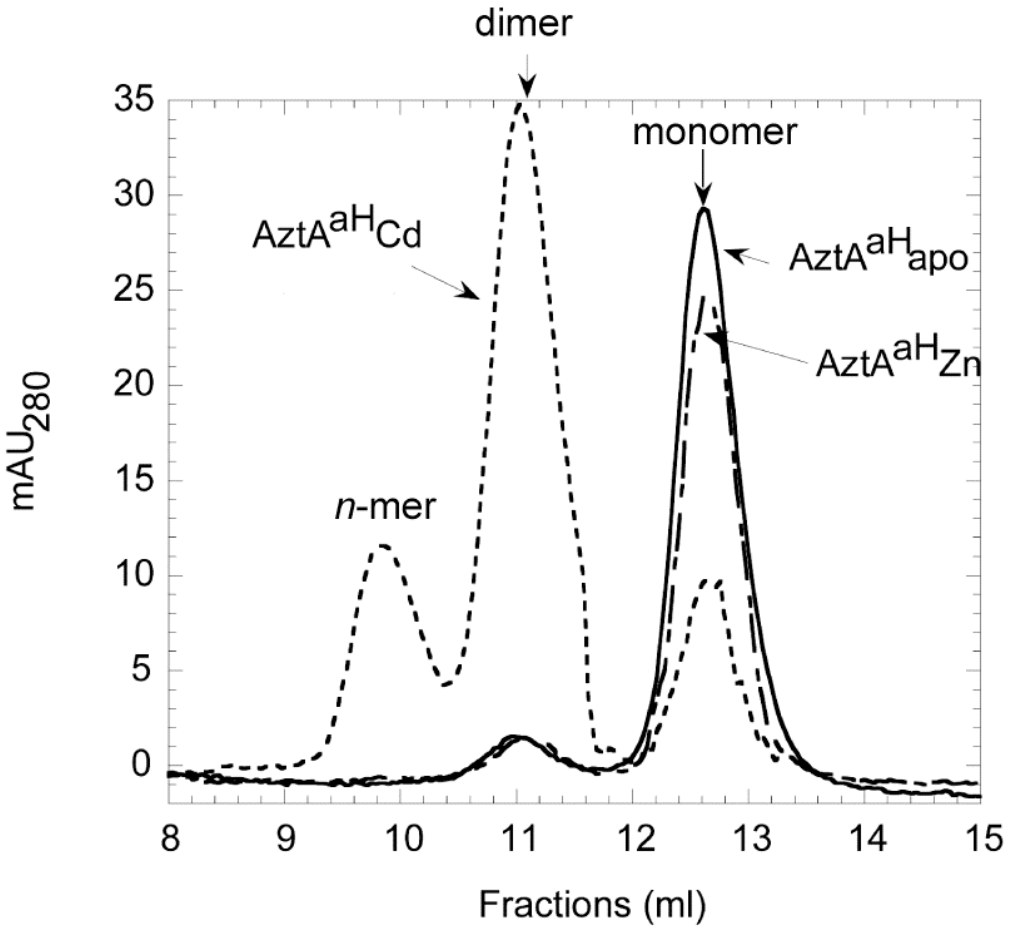

SUPPLEMENTARY FIGURE S1: HPLC size exclusion chromatography (Superdex-75) analysis of apo- (—) vs. Zn_1 (— - —) and $Cd_{0.5}$ (----) forms of $AztA^{aH}$ following ≥12 h incubation of protein with metal ion. The R_g values for the peaks labeled monomer and dimer are 4.85 and 6.5 nm, respectively, as obtained from dynamic light scattering measurements (see Supplementary methods). If the chromatography is carried out immediately after addition of stoichiometric Zn(II) to $AztA^{aH}$, more dimer is observed which interconverts to monomer upon extended incubation; the same is not true for Cd (data not shown).

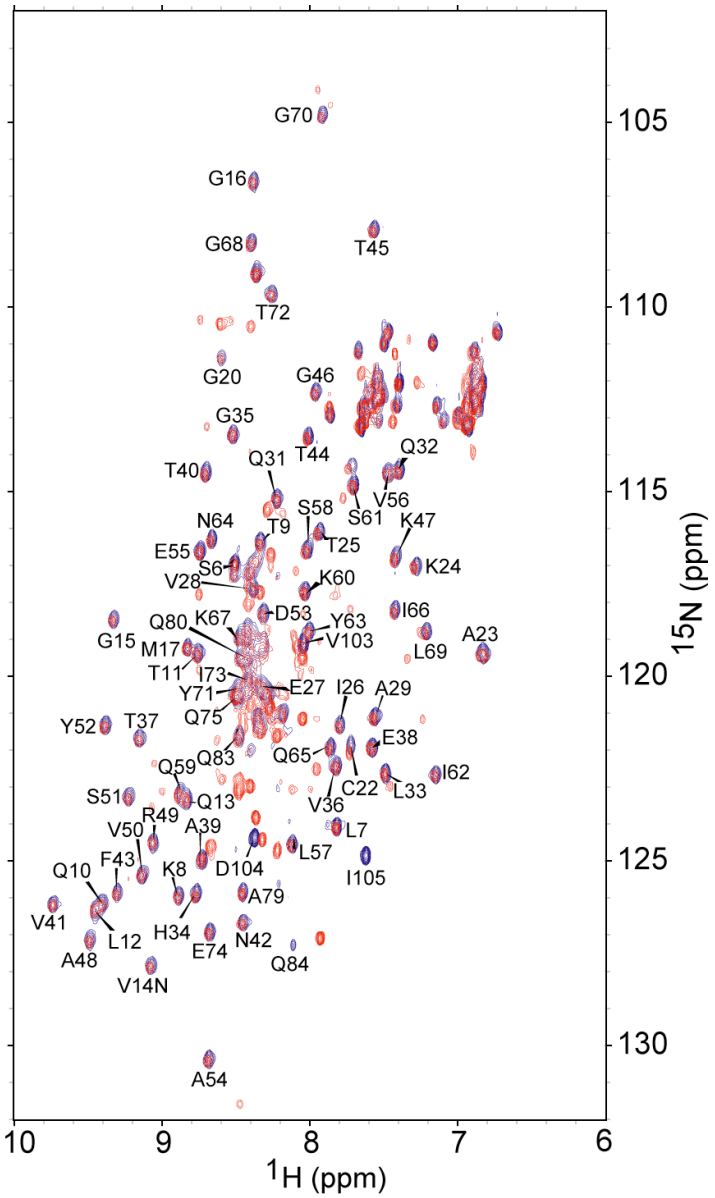

SUPPLEMENTARY FIGURE S2: Overlay of ^{1}H-^{15}N HSQC spectra acquired for apo-AztA^{aH} (*blue contours*) and apo-AztA^{aHbH} (*red contours*) (25 ºC, pH 6.5). Resonance assignments are shown for the a-MBD.

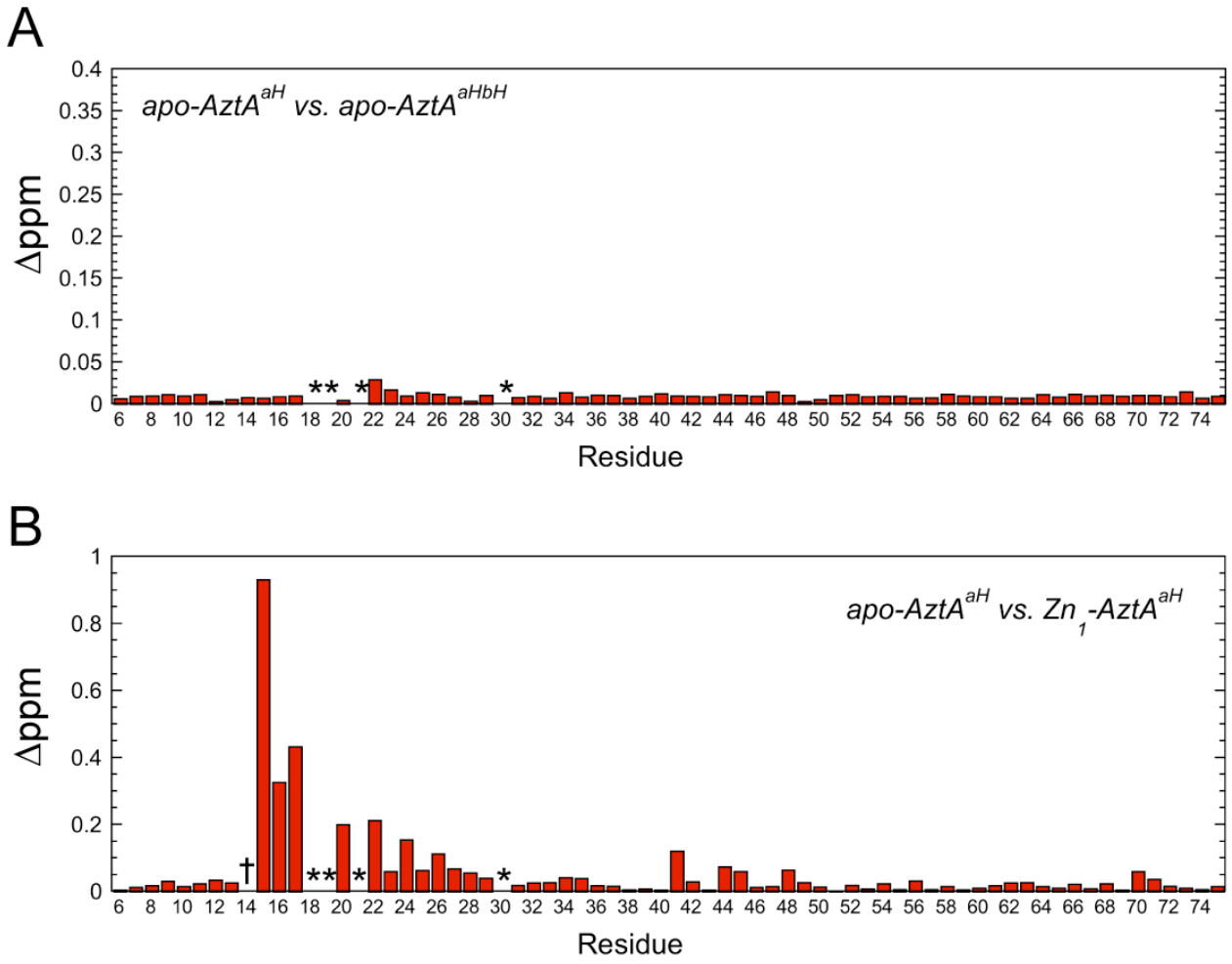

SUPPLEMENTARY FIGURE S3: Chemical shift difference plots (Δppm vs. residue number) for (**A**) apo-AztA^{aH} – apo-AztA^{aHbH} and (**B**) apo-AztA^{aH} – Zn_1-AztA^{aH}. *, unassigned NH resonances in apo-AztA^{aH}; †, unassigned in Zn_1-AztA^{aH}. Δppm = sqrt[(Δppm $^1H)^2$ – (Δppm $^{15}N/7)^2$)]|

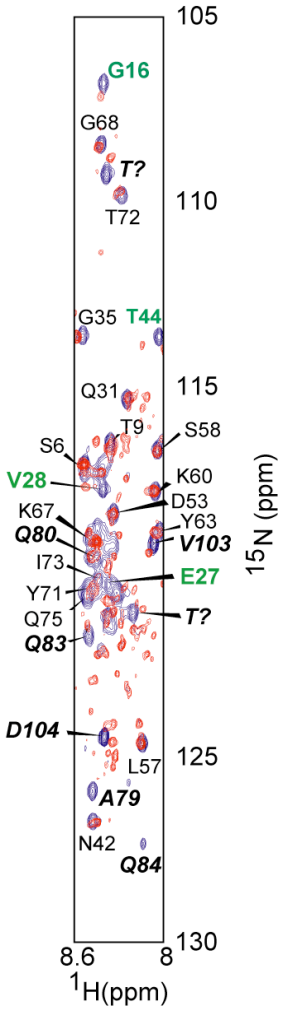

SUPPLEMENTARY FIGURE S4: Subsection of the random coil region of ^{1}H-^{15}N HSQC spectra acquired apo-AztA^{aH} (*blue* contours) and Zn_1-AztA^{aH} (*red* contours). Peaks are designated as follows: *Normal typeface*, resonances in the βαββαβ domain that do not shift significantly on Zn(II) binding (see Fig. S3); *green, bold typeface*, crosspeaks in the βαββαβ domain that shift significantly upon Zn(II) addition (Fig. S3); *bold italicized typeface*, tentatively assigned (#) and unassigned (***T?***) crosspeaks from the unstructured His-rich tail region (residues 76-105) that shift or broaden on addition of stoichiometric Zn(II) to apo-AztA^{aH} (25 ºC, pH 6.5).

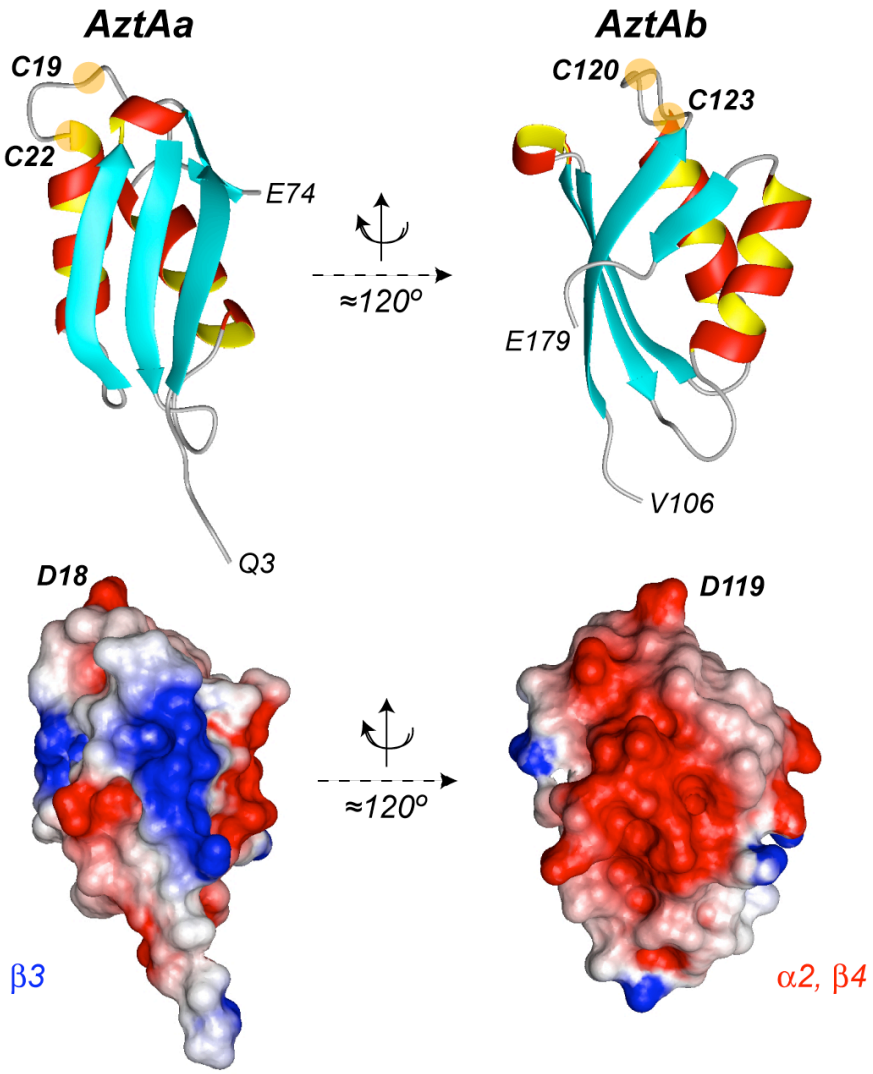

SUPPLEMENTARY FIGURE S5: Electrostatic surface potential renderings of homology models of a-MBDs and b-MBDs of AztA using Swiss-Model (http://swissmodel.expasy.org//SWISS-MODEL.html) and *B. subtilis* CopAa (pdb code 1OPZ) as template. These figures were prepared using Molmol (*7*).

REFERENCES

1. Ankudinov, A. L., Ravel, B., Rehr, J. J., and Conradson, S. D. (1998) Real-space multiple-scattering calculation and interpretation of x-ray-absorption near-edge structure. *Phys Rev B 58*, 7565-7576.
2. Brown, I. D., and Altermatt, D. (1985) Bond-Valence Parameters Obtained from a Systematic Analysis of the Inorganic Crystal-Structure Database. *Acta Cryst Sec B-Structural Science 41*, 244-247.
3. Zeng, Q. D., Lewis, L. M., Colangelo, C. M., Dong, J., and Scott, R. A. (1996) A transcription factor IIB homolog from the hyperthermophilic archaeon *Pyrococcus furiosus* binds Zn or Fe in N-terminal Cys(4) motif. *J Biol Inorg Chem 1*, 162-168.
4. Bonomi, F., Burden, A. E., Eidsness, M. K., Fessas, D., Iametti, S., Kurtz, D. M., Jr., Mazzini, S., Scott, R. A., and Zeng, Q. (2002) Thermal stability of the [Fe(SCys)(4)] site in Clostridium pasteurianum rubredoxin: contributions of the local environment and Cys ligand protonation. *J Biol Inorg Chem 7*, 427-436.
5. Colangelo, C. M., Lewis, L. M., Cosper, N. J., and Scott, R. A. (2000) Structural evidence for a common zinc binding domain in archaeal and eukaryal transcription factor IIB proteins. *J Biol Inorg Chem 5*, 276-283.
6. Banci, L., Bertini, I., Ciofi-Baffoni, S., Su, X. C., Miras, R., Bal, N., Mintz, E., Catty, P., Shokes, J. E., and Scott, R. A. (2006) Structural Basis for Metal Binding Specificity: the N-terminal Cadmium Binding Domain of the P1-type ATPase CadA. *J Mol Biol 356*, 638-650.
7. Koradi, R., Billeter, M., and Wuthrich, K. (1996) MOLMOL: a program for display and analysis of macromolecular structures. *J Mol Graph 14*, 51-55, 29-32.